Can Terrestrial Laser Scanner (TLS) and hemispherical photographs predict Tropical Dry Forest Succession with liana abundance?

G. Arturo Sánchez-Azofeifa[a*], Mauricio Vega-Araya[b], J. Antonio Guzmán Q.[a], Carlos Campos-Vargas[a], Sandra M. Durán[a], Nikhil D'Souza[a], Thomas Gianoli[a], Carlos Portillo-Quintero[c], Iain Sharp[a]

[a] Center for Earth Observation Sciences (CEOS), Department of Earth and Atmospheric Sciences, University of Alberta, Edmonton, Alberta, Canada T6G 2E3

[b] Laboratorio de Teledetección de Ecosistemas (LabTEc), INISEFOR-Universidad Nacional de Costa Rica, Heredia, Costa Rica, Central America

[c] Department of Natural Resources Management, Texas Tech University, Lubbock, Texas, USA.

[*] Corresponding author**.** Tel. +1-780-4921822; E-mail address:gasanche@ualberta.ca

Abstract

Tropical Dry Forests (TDFs) are ecosystems with long drought periods, a mean temperature of 25^{o}C, a mean annual precipitation that ranges from 900 to 2000 mm, and that possess a high abundance of deciduous species (trees and lianas). What remains of the original extent of TDFs in the Americas remains highly fragmented and at different levels of ecological succession. It is estimated that one of the main fingerprints left by global environmental and climate change in tropical environments is an increase in liana coverage. Lianas are non-structural elements of the forest canopy that eventually kill their host trees. In this paper we evaluate the use of a Terrestrial Laser Scanner (TLS) in combination with hemispherical photographs (HPs) to characterize changes in forest structure as a function of ecological succession and liana abundance. We deployed a TLS and HP system in 28 plots throughout secondary forests of different ages and with different levels of liana abundance. Using a canonical correspondence analysis, we addressed how the VEGNET and HPs could predict TDF structure. Likewise, using univariate analysis of correlations we show how the liana abundance could affect the prediction of the forest structure. Our results suggest that TLS and HPs can predict differences in the forest structure at different successional stages, but that these differences disappear as liana abundance increases. Therefore, in well-known ecosystems such as the tropical dry forest of Costa Rica, these biases of prediction could be considered as structural effects of liana presence. This research contributes to the understanding of the potential effects of lianas in secondary dry forests and highlights the role of TLS combined with HPs to monitor structural changes in secondary TDFs.

1 Introduction

Lianas, woody vines, are a key structural component of tropical forests; they account for 25–40% of the woody stems and more than 25% of the woody species (*Schnitzer and Bongers, 2011*). Lianas are structural parasites that use trees to ascend to the forest canopies and move from tree to tree. Lianas have been defined as hyper-dynamic elements of the canopy structure (*Phillips et al. 2005, Sánchez-Azofeifa and Castro, 2006*). Lianas can be detrimental to host trees by competing with them for above- and belowground resources (*Chen et al., 2008*), reducing tree growth rates, and increasing tree mortality (Schnitzer and Carson 2010, *van der Heijden et al., 2013*).

In the last two decades lianas have increased in density and biomass in old-growth forests (*Phillips et al., 2002; Schnitzer and Bongers, 2011*), and this increment is considered to be one of the major structural changes in tropical forests (*Phillips and Lewis, 2014*). These structural changes mentioned above may have potential negative effects on carbon stocks since they tend to reduce carbon storage and uptake in old-growth tropical forests (*Durán and Gianoli, 2013; van der Heijden et al., 2015*). Liana dynamics in secondary forests and their impact on forest structure, however, are not yet understood despite the fact that secondary forests are becoming increasingly dominant in tropical regions, and currently occupy more area than old-growth forests (*Durán and Sánchez-Azofeifa, 2015; Wright, 2005*).

Lianas are considered light-loving plants, because they tend to respond positively to disturbance and show high density in areas of secondary forest succession (*Paul and Yavitt, 2011*). Furthermore, secondary forests may promote liana abundance because they provide both high light availability and an abundance of trellises (*Schnitzer and Bongers, 2002*). As

62 tree turnover increased gaps due to mortality, lianas can take advantage of this process and
63 form dense tangles, which in turn reduce the amount of light reaching the forest understory
64 (*Paul and Yavitt, 2011; Schnitzer et al., 2000*). These liana tangles can persist for long
65 periods (up to 13 years) and alter the successional pathway stalled by liana abundance by
66 inhibiting the regeneration, growth, and density of late successional species (*Schnitzer et al.,*
67 *2000*).

68 As of today, it is still unknown whether lianas can alter successional trajectories in
69 secondary forests resulting from anthropogenic disturbance (*Durán and Sánchez-Azofeifa,*
70 *2015*). Two studies in secondary wet forests have found an increment in liana density in the
71 first 20 years of regeneration (age since land abandonment), with a subsequent decline
72 (*DeWalt et al., 2000; Letcher and Chazdon, 2009*). This decline of lianas in wet forests
73 appears to be related with reductions in light availability due to greater tree and shrub
74 biomass at later stages of succession (*Letcher and Chazdon, 2009*). Nonetheless, it remains
75 unclear whether this pattern holds true with more open forest types, and whether other
76 factors such as structure, canopy openness, plant density and the volume of forest stands can
77 also influence successional trajectories of lianas (*Durán and Sánchez-Azofeifa, 2015;*
78 *Sánchez et al., 2009*).

79 Despite the fact of the important effect of lianas on the biomass distribution within
80 tropical forests (*Schnitzer and Bongers, 2011; Ledo et al. 2016*), and their potential role as
81 fingerprints of climate change (Phillips et al. 2005), remote sensing tools aimed to measure
82 their presence/absence as well as their distribution within tropical forests are limited (*Foster*
83 *et al., 2008, Kalacksa et al. 2007a & b, Zhang et al. 2006*). Current knowledge based on leaf
84 spectroscopy approaches provides two key messages regarding liana extent mapping: first

85 that lianas in tropical rainforests tend to confuse the spectral reflectance of their host trees
86 making it in many cases impossible to use remote sensing to create species maps (*Castro-*
87 *Esau et al., 2004)*, and second that there is a higher degree of probability of success for
88 efforts aimed to map liana coverage in tropical dry forests than on rain forests environments
89 (*Sanchez-Azofeifa et al., 2009b; Kalacska et al. 2007b)*.

90 Moreover, studying the impact of lianas on tropical dry forest structure, *Sanchez-*
91 *Azofeifa et al*. (*2009*) used hemispherical photography over a succession of tropical dry
92 forests in Mexico, Costa Rica and Brazil, found that lianas infested sites were significantly
93 different in both canopy openness and Woody Area Index (WAI). Findings associated to
94 WAI impacts were significant since this structural variable when associated to Leaf Area
95 Index (LAI), is used to defined the concept of Plant Area Index (PAI = LAI + WAI).

96 Initial attempts aimed to start untangling the effects that lianas have on remote
97 sensing observations may require data fusion techniques on which hyperspectral remote
98 sensing approaches (leaf spectroscopy finding) are mergered with ground based forest
99 structure information derived from terrestrial laser scanners and hemispherical photography
100 (e.g. LAI, WAI and PAI). Terrestrial Laser Scanners (TLS) have demonstrated their capability
101 to measure canopy properties such as height and cover (*Ramírez et al., 2013*) and tree
102 architecture (*Lefsky et al., 2008*), (*Dassot et al., 2011*; *Richardson et al., 2014*). In the last
103 decade, there has been a rapid development in portable TLS (*Dassot et al., 2011; Richardson*
104 *et al., 2014*). When laser pulses emitted in the visible or near-infrared come into contact with
105 an object, part of that energy is reflected back toward the instrument which triggers the
106 recording of its distance and intensity (*Beland et al., 2014*). TLS systems typically employ
107 vertical and horizontal scanning around a fixed point of observation, providing a

hemispherical representation of biomass distribution in the forest -leaves, branches and trunks- which allows for the exploration of foliage angle distributions and clumping (*Clawges et al., 2007; Jupp et al., 2009; Strahler et al., 2008*).

Until today, there has been no concrete evidence about how liana abundance can affect the prediction of the forest structure by TLS or hemispherical photographs (HPs), which in turn can drive the development of better remote sensing techniques for mapping their extent. Because of this, the objective of this study was to evaluate the feasibility of a TLS named VEGNET in combination with HPs to assess changes in forest structure in secondary TDFs with different levels of lianas abundance. The VEGNET is a TLS that automatically scans a forest plot producing a vertical foliage density profile. Given its automated mode of operation and semi-permanent installation, the VEGNET instrument is described as an *in situ* Monitoring LiDAR (IML) (*Culvernor et al., 2014; Portillo-Quintero et al., 2014*).

As such, in this paper we first assess the potential of VEGNET and HPs to detect the vertical structure of forest stands at different successional stages. Second, we examine how liana abundance could affect the bias of prediction of VEGNET and HPs to detect the level of succession of a given forest stand. Therefore, in well-known ecosystems such as the tropical dry forest of Costa Rica, this bias of prediction could be considered as the effect of liana presence on forest structure.

2 Methods

2.1 Study Area

130 The study area is located in the Santa Rosa National Park Environmental Monitoring Super
131 Site (SRNP-EMSS), which is a part of the Guanacaste Conservation Area in Costa Rica
132 (10°48" N, 85°36" W) (Figure 1). This site covers an area of 50,000 ha, receives 1720 mm
133 of annual rainfall, has a mean annual temperature of 25°C and a 6-month dry season
134 (Dec–May) (*Kalácska et al.,2004*). The SRNP-EMSS site has suffered intense deforestation
135 in the past 200 years due to the expansion of pasturelands (Calvo-Alvarado et al., 2009).
136 Original land management practices in the park included pasture rotation between different
137 large corrals surrounded by life fences that can still be identified today. More recently (early
138 1970's) with the creation of Santa Rosa National Park, a process of secondary regeneration
139 has become the dominant land cover change force in the region. Today and after the creation
140 of SRNP, the uplands of the park are a mosaic of secondary forest in various stages of
141 regeneration and with different land use histories related to anthropogenic fires, intense
142 deforestation, and clearing for pasture lands (*Kalácska et al., 2004; Arroyo-Mora et al.,*
143 *2005a, Cao et al, 2015*).
144
145 **2.2 Definition of forest cover and plot age.**
146 A map of forest cover and forest cover ages was generated using aerial photographs
147 collected by the US Army in 1956 (Scale 1:24,000), a Multispectral Scanner (MSS) image
148 from 1979 (80 m spatial resolution); 4 Landsat Thematic Mapper [TM] images from 1986,
149 1997, 2000 and 2005 (28.5 m spatial resolution); one Spot Multispectral image from 2010
150 (20 m spatial resolution); and a Landsat 8 image from 2015. All images had less than 10%
151 cloud cover.

152 The 1986 image was georeferenced to 1:50,000 topographic maps from the Costa Rica
153 National Geographic Institute with a Root Mean Square Error (RSME) of 0.5 pixels or 14.25
154 m. We defined this as our master image in order to georeference all of the other images, as
155 such all other images were then geo-referenced to the 1986 image seeking a RMSE close to
156 0.5 pixels between the master and the target image. All images where then classified using a
157 supervised classification. Image accuracy was conducted for the 1997, 2000, 2005 and 2010
158 satellite images as part of independent validation efforts conducted by the Costa Rica's
159 National Forest Financing Fund (FONAFIFO). Overall accuracy for the forest/non-forest
160 images was 90%. Further information on image processing can be found in Sánchez-
161 Azofeifa et al. (2001).
162 Final quality controlled forest cover maps (forest non-forest) for 1956, 1979, 1986, 1997,
163 2000, 2005, 2010 and 2015 were cross referenced to produce a tropical dry forest age map.
164 Specifically, forest coverage with 60 years old correspond to woodlands which were being
165 observed in images since 1956; forests that were 40 years old were not detected in 1956 but
166 have been recognizing as forests since 1979; on the other hand, woodlands that were referred
167 to as being 10 years old have a minimum of 10 years as a discriminable forest coverage.
168 Based on Arroyo-Mora et al. (2005b) and Kalascka et. al's (2005a) studies the following
169 successional classification was developed: Ages 10 to 40 years (Early), and ages 40 to 60
170 (Intermediate). Figure 1 presents the final land cover and forest age map for our study area.
171
172 **2.3 Plots selection and description**
173 Based on Figure 1, twenty-eight randomly stratified 0.1ha plots were selected. The number
174 of plots chosen for each forest successional stage was based upon each stages total forest cover

175 area. Plot sizes of 0.1 ha follows convention used in tropical forest studies at this site (Kalascka
176 et al. 2005a). Fieldwork conducted in July 2016 was conducted in order to characterize
177 diameter at breast height (DBH), tree height, total biomass, VEGNET observations (canopy
178 vertical profiles) and hemispherical photos (Canopy openness and Leaf Area Index).
179 The characterization of successional stages was performed following previous approaches
180 for seasonally dry forests of Costa Rica (*Arroyo-Mora et al., 2005b; Kalácska et al., 2005*) and
181 adjusted according to the estimated forest ages (Figure 1). These approaches categorized the
182 secondary regeneration in different successional stages such as early and intermediate
183 successional stages (*E* and *I*, respectively) (*Arroyo-Mora et al., 2005a*). The *E* stage is a
184 forest area with patches of sparse woody vegetation composed of shrubs, small trees, and
185 saplings, with a thick herbaceous understory, and with a single stratum of tree crowns with a
186 maximum height of less than 10 m (*Castillo et al., 2012*). Some of the common species that
187 are characteristic of this early stage of succession includes *Genipa americana*,
188 *Cochlospermum vitifolium*, *Gliricidia sepium*, *Randia monantha* (*Hilje et al., 2015;*
189 *Kalácska et al., 2004*). In contrast, the *I* stage has two vegetation strata composed of
190 deciduous species of woody plants. The first strata is comprised of fast-growing deciduous
191 tree species that reach a maximum height of 10–15 m (e.g., *Cydista aequinoctialis*) and the
192 second stratum is represented by lianas and vines, adults of shade-tolerant and slow-growing
193 evergreen species as well as the juveniles of many species such as *Annona reticulata*,
194 *Ocotea veraguensis*, and *Hirtella racemosa* (*Arroyo-Mora et al., 2005a; Kalácska et al.,*
195 *2004*). No lianas were present in the early successional stage plots. Lianas in early forests
196 tend to be more present during the transition from early to intermediate stages. We did not
197 select “late forests” at our study site since they tend to reflect structural characteristics

198 (DBH, three height and species composition) associated tropical moist forest (Tosi, personal
199 communication).
200 On the other hand, the characterization of the plots according to the liana abundance was
201 based on the structure of plants that compose the tropical dry forest of SRNP-EMSS. In this
202 way, we classified the 28 plots according to the relative abundance of stems of lianas over
203 total number of stems, where plots with a relative abundance greater than 0.1 were
204 categorized as plots having high liana abundance (HL), while plots with a relative
205 abundance lower than 0.1 were categorized as having a low liana abundance (LL). Although
206 this classification seems to be in-deterministic, this kind of classification represents an
207 important ecological component which is very difficult to study as a continuum due to its
208 spatial and temporal variation, and its categorization can help to improve the understanding
209 of ecological processes as many other ecological categories.
210 At the end of this characterization, ours plots for the study consisted of 5 *E*-LL plots, 6
211 *E*-HL plots, 7 *I*-LL plots, and 10 *I*-HL plots. In each of these plots we extracted the available
212 information that described the complexity of the dry forest according to its structure, but at
213 the same time deployed the ground LiDAR and hemispherical photograph measurements to
214 predict and describe that complexity. Information about the parameters used and estimated
215 according to the forest structure, ground LiDAR, and hemispherical photographs is
216 described below.
217
218 **2.4 Forest structure**
219 Four parameters that characterize the forest structure were used in this study. These
220 parameters were selected because these are easily obtained in any forest inventory, which

could help in the applicability of this study in other regions. Specifically, we selected the stem density (stems/ha) as a parameter to describe the number of individuals per plot, the mean diameter at breast height (1.3 m) (DBH_{mean}, cm) as a parameter that can describe the mean size of the individuals, the total basal area (TBA, m^2) as a parameter that can describe the biomass of each plot, and the ratio of liana basal area to TBA (L/TBA) as a parameter that can describe the contribution of lianas biomass to the total biomass of each plot. Each of these parameters was extracted from DBH measurements for lianas (>2.5 cm) and trees (>5 cm).

2.5 Ground LiDAR measurements

The VEGNET ground LiDAR system was deployed in the middle of each of the selected plots, in which a single successful scan was performed between June 12th to June 27th, 2016. The VEGNET IML instrument uses a phase-based laser rangefinder with a wavelength of 635 nm, in which a laser beam is directed at a rotating prism that reflects the laser at a fixed angle of 57.5° zenith or the "hinge angle" (*Jupp et al., 2009*). The prism is designed to perform full 360° azimuth rotations at this fixed zenith angle (no vertical scanning motion) and has the capability to be programmed to obtain up to 7360 range measurements for a full azimuth scan (an average of 20.6 measurements per azimuth degree) (*Culvenor et al., 2014*). Because sunlight irradiance may cause interference with the VEGNET laser at the same wavelength (*Culvenor et al*., 2014, *Portilllo-Quintero et al*., 2014), measurements for the VEGNET were conducted at night. Some tests of the measurement process by VEGNET at night time indicated that at distances greater than 60 m or in areas larger than 3600 m^2 (0.36 ha) the laser beam does not provide reliable measurements (*Culvenor et al., 2014*). In a

tropical forest setting, data analysis and interpretation may be restrained to the footprint, which is dependent on forest height at each site. Based on the forest heights of our study sites, the effective footprint of LiDAR measurements was within 0.1ha of our original sampling area.

From these measurements at night six parameters were estimated: the maximum tree height (H_{max}), the plant area index (PAI), plant area volume density (PAVD), the centroid of x (C_x) and y (C_y), and the radius of gyration (RG). To estimate these parameters, the height (h) was initially calculated as the cosine of the laser zenith angle (57.5°) multiplied by the laser distance measurement (d) assuming that the terrain is flat as describe *Culvenor et al. (2014)*.

On the other hand, canopy "hits" and "gaps" were recorded to enable the calculation of angular gap fraction or gap probability (P_{gap}) at each h where a leaf, trunk or branch was hit by the laser (*Lovell et al., 2003*). P_{gap} at a given h is the ratio of the number of valid returns below z ($\#z_i < h$) to the total number of laser shots (N) (*Culvenor et al., 2014*):

$$P_{gap(z)} = [\#z_i < h\ ] / N \quad (1)$$

Consequently, the estimation of cumulative plant area index (PAI) by the conversion of $P_{gap(z)}$ was performed using the following the equation (*Culvenor et al., 2014*):

$$PAI_{(z)} = -1.1 \times \ln(P_{gap(z)}) \quad (2)$$

From this calculation, the density of vegetation components at any level of z was computed as the derivative of PAI with respect to h. This calculation is commonly referred to as the plant area volume density (PAVD) (*Culvenor et al., 2014*) described by:

$$PAVD_{(z)} = \delta\, PAI_{(z)} / \delta_z \quad (3)$$

It is important to note that these calculations represent tridimensional variations (x, y, z) of the forest structure (*Culvenor et al., 2014*), because of this, in our statistical analysis we used the maximum h estimated by the LiDAR per plot (H_{max}), the cumulative PAI as a function of the canopy height (PAI), and the mean PAVD at different heights ($PAVD_{mean}$). These calculations were extracted using the "VEGNET Data Display and Export Version 2.5" software developed by Environmental Sensing Systems Inc (Melbourne, Australia).

Likewise, from the LiDAR measurements we also used shape metrics such as the centroid (C) and radius of gyration (RG) to understand how the vertical profile of the forest could change according to successional stages and liana abundance. The RG and the C are metrics that are mainly used in LiDAR waveforms to describe the motion of objects and the manner in which material is distributed around an axis (*Muss et al., 2013*). We used a similar approach by calculating the C and the RG for the PAVD vertical profile of each plot. Specifically, C represents the geometric center of a two-dimensional (x and y) region (e.g., the arithmetic mean position) of all the points (n) in the shape of the PAVD profile and it could, specially, be interpreted as the variability of PAI with height and it will change as a function of understory changes along the path of succession (grasses to shrubs to short

trees). On the other hand, RG is the root mean square of the sum of the distances for all points on the PAVD vertical profile, which is described as:

$$RG = \sqrt{\frac{\sum(x_i - C_x)^2 + \sum(y_i - C_y)^2}{n}} \quad (4)$$

This parameter can be visualized as the relationship between the total length of the PAVD vertical profile and its shape and position, which are determined using the sum of *x* or *y* coordinates divided by the total length of the profile (*Muss et al., 2013*). In general, the RG captures the manner in which the PAVD profile is distributed around the centroid, making it a better descriptor of the vertical profile shape than just the centroid itself, and thus, more suitable for relating VEGNET measurements to forest structure (*Muss et al., 2013; Culvenor et al., 2014*). Therefore, we used the RG to relate the shape of the PAVD profile to forest biomass at the footprint level For a more detailed explanation on the functioning of the VEGNET in the field please refer to *Portillo-Quintero et al*. (*2014*) as well as *Culvenor et al.* (*2014*). A single successful scan was performed during the wet season using the VEGNET instrument at each site on clear nights.

2.6 Hemispherical photographs

Hemispherical photographs (HPs) were taken during the early morning in the middle of each plot, using a digital camera (E4500, Nikon, Tokio, Japan) equipped with a fisheye lens of 35 mm focal length. The camera was leveled at 1.50 m by a tripod and orientated towards magnetic north, in order to ensure photographic standardization. The resulting pictures were analyzed using the software Gap Light Analyzer version 2.0.4 (*Frazer et al., 1999*). This

311 analysis was performed by creating 340 sky sectors (36 azimuth classes and 9 elevation
312 angle classes) with a time series of 2 min along the solar track. The leaf area index (LAI)
313 and the canopy openness were subsequently extracted by this analysis; however, the LAI
314 was extracted using the "4 ring" (with a zenith angle between 0 to 60º) which is a more
315 accurate depiction of the site than using "5 rings" because the latter takes into account trees
316 that are not immediately surrounding the site, and which are found outside of the plot
317 footprint.
318
319 **2.7 Statistical analysis**
320 This study compared the effect of the successional stages, the abundance of lianas, and their
321 interaction on the parameters of forest structure as well as VEGNET-HPs parameters using a
322 multivariate analysis of variance (MANOVA), in order to demonstrate that this study had
323 been conducted in contrasting environments. For each MANOVA we extracted the
324 univariate analysis of variance (ANOVA) to describe the multivariate effects of each
325 parameter. To show the potential of the VEGNET and HPs to predict variations in the
326 structure of the dry forest, we applied a canonical correlation analysis (CCA) using the
327 VEGNET-HPs parameters as independent variables and the features of the forest stand as
328 dependent variables. Due to the CCAs sensitivity to the collinearity among variables (*Quinn*
329 *and Keought, 2002*), we only used RG, PAI, $PAVD_{mean}$, H_{max}, LAI, and canopy openness as
330 independent parameters. Specifically, the CCA was used to extract the canonical correlation
331 between VEGNET-HPs and forest structure (eigenvalues), the correlation between the
332 canonical variates and each matrix (eigenvectors), and the scores that describe the
333 multidimensional variation of each plot according to its correlation. To extract the statistical

significance of the canonical correlation coefficients, we computed an asymptotic test on the first canonical dimensions to extract the *F*-approximations of Wilks' Lambda along with its significance. This statistical significance was subsequently validated using a permutation test on each dimension by 10000 iterations.

After describing the potential of the VEGNET-HPs parameters to predict variations in the structure of the dry forest, we were interested in demonstrating how the relative abundance of lianas could affect the bias of prediction extracted from these sensors. In ecological terms, it is a perceived expectation that during successional transitions increases in basal area, height and vertical strata of the vegetation should be observed; consequently, these transitions could be translated into increases in VEGNET-HPs parameters (except canopy openness which is inverse). However, from hypothesis derived from previous studies, it is possible that the abundance of lianas may actually arrest the forest succession and reduce the biomass accumulation of woody vegetation (*Paul and Yavitt 2011; Schnitzer et al., 2000*). If the above is true, correlations between descriptors of forest structure and parameters extracted from VEGNET and HPs could be diffuse or stochastic in the dry forest, and their application under the presence of lianas could prove ineffective. Under this reasoning, we compare the parametric correlations of four parameters according to the successional stages and the liana abundance, separately. The four parameters selected were those with the two highest correlation values for the VEGNET-HPs matrix and the two parameters with the highest correlation values for forest structure, determined by the first two canonical dimensions described by the CCA. This comparison was conducted using an ordinary resampling method to replicate the correlation 5000 times, in which the resampled

values were used to build density plots to describe the bias of prediction according to its overlap.

The previous analyses were conducted in R software version 3.3.1 (R Development Core Team, 2016) using the "CCA" package (*González and Déjean, 2015*) to extract the canonical correlations, the "CCP" package (*Menzel, 2009*) to extract the significance of the CCA and its permutation, and the "boot" package (*Canty and Ripley, 2016*) to extract the resampled values. When the normality of the data was not reached, each parameter was previously transformed using the Box-Cox transformation for the analysis.

3 Results

3.1 Changes on forest structure along the path of succession and liana abundance

According to the MANOVA the forest structure of our plots differed between successional stages (Wilk's $Lambda_{(4,21)} = 0.51$; $p < 0.01$) and liana abundance (Wilk's $Lambda_{(4,21)} = 0.58$; $p < 0.05$), but without interaction between these categories (Wilk's $Lambda_{(4,21)} = 0.76$; $p = 0.20$). This analysis suggests that the DBH_{mean} and TBA were the only parameters affected by the interaction between successional stages and liana abundance, where *E* successional plots with LL and *I* plots with HL showed lower values of DBH_{mean} and TBA than *E* and *I* plots with HL and LL, respectively (Table 1). In terms of the effect of the liana abundance, the univariate analysis suggests that plots with LL showed lower values of L/TBA in comparison with HL plots.

3.2 VEGNET-Hemispherical Photographs (HPs), forest succession, and liana abundance

379 The multivariate comparisons of the VEGNET-HPs parameters showed that the sensor
380 estimations did not differ between successional stages (Wilk's $Lambda_{(8,17)} = 0.58$; $p =$
381 0.21), liana abundance (Wilk's $Lambda_{(8,17)} = 0.62$; $p = 0.29$), and these categories did not
382 show an interaction (Wilk's $Lambda_{(8,17)} = 0.53$; $p = 0.14$). Despite the absence of a
383 multivariate effect of the liana abundance, the univariate responses extracted from this
384 comparison suggest that the LAI and canopy openness differs between plots with HL and
385 LL, where LL plots showed lower values of LAI and higher values of canopy openness in
386 comparison with HL plots (Table 2). On the other hand, the univariate responses showed
387 that the canopy openness was affected by the successional stages, where *E* successional plots
388 showed higher values of canopy openness than *I* plots. Likewise, the univariate comparisons
389 suggest that C_x, PAI, and $PAVD_{mean}$ are affected by the interaction of the successional stages
390 and liana abundance, where *E* successional plots with LL and *I* plots with HL showed higher
391 values of C_x, PAI, and $PAVD_{mean}$ in comparison with *E* and *I* successional plots with HL and
392 LL, respectively.
393
394 **3.3 Canonical correspondence analysis and trends of forest structure**
395 The CCA showed that sensor parameters are strongly associated with the trends in forest
396 structure (Fig 2). In general, the first and second canonical dimension showed correlations of
397 0.81 (Wilk's $Lambda_{(24,64.01)} = 0.13$; $p < 0.01$) and 0.72 (Wilk's $Lambda_{(15,52.85)} = 1.46$; $p =$
398 0.16) between our sensors and forest structure. Specifically, the correlation between the
399 canonical variates in the first canonical dimension suggested that canopy openness and the
400 LAI have a great weight in the sensor matrix, while L/TBA and stem density had an
401 important effect on the forest structure (Fig 2a). Likewise, the correlation between the

canonical variates in the second canonical dimension showed that H_{max} and $PAVD_{mean}$ had a strong correlation with the sensor parameters, while TBA and steam density had a strong correlation on the forest structure. The scores that described the multidimensional variation of each plot did not reflect a visual aggregation according to the successional stages and liana abundance (Fig. 2b). In terms of the validation of the significance of the canonical correlation coefficients, the permutations test showed that there is an important increase in the significance of the first two canonical dimensions (Fig. 2c, 1d), where the first dimension presented an increase of 0.21 points for the Wilks's statistic, while the second dimension showed an increase of 0.25 points, which results in a significant effect.

3.4 Comparison of correlations between successional stages and liana abundance

The different trends of correlation showed that the successional stages and mainly the liana abundance have an important effect in the prediction of the forest structure using VEGNET-HPs parameters (Figure 3), but at the same time, these trends showed that some of these parameters have the potential to predict the implication of the liana abundance on the forest structure. Specifically, variation in the correlations of canopy openness on L/TBA (Figures 3a, b, c) and H_{max} on TBA (Figures 3g, h, i) showed that the correlation trends between successional stages are overlapped, while the correlations trends between liana abundance are separated, in where low values of canopy openness and H_{max} are associated with high values of L/TBA and TBA, and consequently with the discrimination of HL plots. Likewise, variation in the correlation between LAI and L/TBA showed that the trends might not be used to separate successional stages or liana abundance (Figures 3d, e, f). However, the correlation between H_{max} and TBA suggest that H_{max} can not discriminate between different

successional stages, but can discriminate with different liana abundance (Figures 3j, k, l), where lower values of correlation are associated with HL plots.

4 Discussion

4.1 Potential of VEGNET and HPs to detect the vertical structure of forest stands at different successional stages

Woody vines or lianas tend to proliferate in disturbed forest stands such as regenerating forests (*Paul and Yavitt, 2010*). Much research on liana ecology, however, has focused on old-growth forests despite that secondary forests currently cover a larger area than old-growth forests and may become the dominant ecosystem in tropical regions (*Wright, 2005*). Due to shorter stature and a higher variability of light in secondary forests, lianas may be particularly abundant in these ecosystems, but little is understood about the role of lianas in forest succession (*Letcher and Chazdon, 2009*). In this study, we used the VEGNET, a terrestrial LiDAR system combined with HPs, to assess the impact of liana abundance on forest succession. Our overall analysis indicated that VEGNET parameters, in combination with HPs derived information, were able to characterize changes in forest structure at different successional stages with and without lianas. Changes observed using HP, along the successional gradient, we similar to those observed in other tropical dry forests environments where parameters such as biomass, LAI, Canopy Openess and H_{max} changed as trees grow (Sanchez-Azofeifa et al. 2009). Our work using the TLS suggested also that this technology can be also used to detect differences along the forest succession trajectory when lianas are integrated into the analysis. In terms of the comparison of VEGNET parameters between our categories, probably the effect of the interaction of the successional

448 stages and liana abundance on C_x, PAI and $PAVD_{mean}$ are some of the most reveling. As
449 lianas emerge along they path of succession they create a more heterogenous space which is
450 captured by the variability on C_x. C_x is affected by PAI and $PAVD_{mean}$ as function of
451 understory components (shurbs, grasses and also liana tangles). A higher value of C_x may be
452 interpreted on an E-LL as a high dominance of shubrs, tall grasses and short trees; while a
453 high value of C_x on a E-HL will mean a high distribution of tangles combined with shurbs
454 which make accessibility impossible to some sites due to a high density of understory liana
455 tangles.
456
457 **4.2 How liana abundance could affect the bias of prediction of VEGNET and HPs to**
458 **detect the level of succession of a given forest stand?**
459 When we consider the bias of correlations between the forest structure and the parameters
460 extracted from our two sensors at different successional stages, as well as liana abundance,
461 our results suggest that this late variable has an important effect on the bias of prediction for
462 a given forest structure. The main reason is probably a result of lianas introducing random
463 tangles into the 3-dimensional space that is occupied by all forest biomass at a given plot. In
464 other words, lianas tend to randomize or reduce the degree of organization of the natural
465 space which is typically utilized by trees. This randomization of the 3D space occupied by
466 trees and lianas is an element that has not been considered as of today; since most studies do
467 not consider the space occupied by lianas because of a lack of TLS information.
468 This change in deterministic patterns of the forest structure is probably due to
469 competition between lianas and trees in forest stands within a random 3D space. In disturbed
470 sites, such as secondary forests, lianas deploy leaves in the canopy and create large amounts

of tangles in both the ground and mid canopy, this high density of tangles contribute to a reduction on the amount of available transmitted incoming solar radiation available for photosynthesis at the understory (Sanchez-Azofeifa et al. 2009, Graham et al., 2013). Moreover, in regenerating stands within forests (e.g., treefall gaps), high densities of lianas can inhibit the regeneration of tree species and reduce the abundance of shade-tolerant trees (*Schnitzer et al., 2000*), which in turn can affect the 3D arrangement of species within a given area. These ecological processes may cause a shift in forest structure, which is detected as a shift in the vertical structure signature by TLS in sites with high liana abundance. These differences in structures have been confirmed in a recent study, which found that a liana-infested forest had a more irregular canopy with canopy heights between 10 and 20 m, while the surrounding forests had a significantly taller canopy between 25 and 35m along with a denser canopy (*Tymen et al., 2016*). Together, our results and Tymen et al. (2016) observations could highlight the potential of entropy analysis of the forests to detect the presence and the effect of lianas on the forest structure and the pathways of succession.

4.3 A cautionary tale associated to emergent TLS monitoring technologies applied to liana-infested sites

Our observations from changes on DBH_{mean}, TBA, LAI and canopy openness as function of liana abundance provide evidence that these variables can be used to estimate the impact of lianas on forest structure along the path of succession, although not all of parameters, such as stem density and L/TBA, were significant. In other words, there is a strong need to carefully select which parameters should be considered if we want to estimate changes in the forest structure as function of liana abundance. One key example is the use of PAI (PAI=

494 LAI + WAI) as tool to evaluate the impact of liana abundance on forest succession. PAI as a
495 single measurement theoretically could provide insights on the impact of liana abundance on
496 successional stages; as such we could expect that PAI will increase as leaf and wood biomass
497 increases during succession (*Quesada et al., 2009*). Furthermore, PAI could be better
498 understood if specific measurements of TLS can be done during the dry season to quantify the
499 real value of WAI to PAI, tropical dry forests in contrast to tropical rainforests can provide
500 significant advantage on better understanding PAI (Kalascka et al. 2005b). It is surprising that
501 we did not find differences in the PAI values between stands that did and did not have
502 lianas. It is possible that PAI is not the best parameter to differentiate between plots with and
503 without liana presence, instead variables more related with leaf components, such as leaf
504 area index (LAI) and Woody Area Index (WAI) may be more suitable for finding
505 differences in liana signature across sites, especially when the contribution of lianas to the
506 woody area index (WAI) to overall plot PAI is relatively small in comparison to the
507 allocation of WAI from trees (Kalascka et al. 2005b, *Sanchez-Azofeifa et al., 2009*).
508 A recent study assessing the role of lianas on forest dynamics in the Amazon,
509 indicated that a liana-infested forest appeared to be in an arrested stage of ecological
510 succession, due to the evidence provided by LiDAR surveys from 2007 to 2012 which
511 showed that the overall extent of forest area had remained stable, with no notable net gain or
512 loss over the surrounding forest (*Tymen et al., 2016*). It is possible that studying forest
513 dynamics in forest stands across successional stages, with different levels of liana abundance
514 integrated into the TLS and HPs parameters, may allow us in the future to provide stronger
515 evidence as to whether lianas can arrest succession in dry forests as it appears to occur in
516 humid forests (*Schnitzer et al., 2000; Tymen et al., 2016*).

Moreover, our work seeks to strength the argument for the inclusion of lianas on global terrestrial vegetation models (*Verbeek & Kearsley, 2016*). We argue here that the first step on the development of such models is to have a clear understanding of how lianas affect ecosystem structure and composition, which in turn, will affect tree mortality/recruitment, and carbon storage aboveground and belowground (*Poulsen et al. 2016, Schnitzer et al. 2014*). Furthermore, lianas because of their impact on the 3D structure of a given forest space, may have the possibility of changing faunal diversity (e.g. birds) an impact that has not fully documented as today. As such, our study also supports the arguments by Schnitzer et al (2016) that calls for the need for developing a network of observational and experimental sites that can provide insights on the impact of lianas at different ecological levels.

We extend the previous argument to remote sensing studies as well. Since lianas represent a significant ecological component of tropical ecosystems (with stronger presence on intermediate stages than early or late successional stages), we also argue that the development of more robust global vegetation models must start from understanding liana impact of forest structure which in turn will drive other components of those models.

5 Conclusions

This study evaluated the potential for TLS and hemispherical photos to observe differences between successional stages of a tropical dry forest chrono-sequence and liana abundance. Our work provided five main conclusions: (1) that TLS data combined with hemispherical photography data can help to predict the forest structure of the tropical dry forest as demonstrated before, (2) that these predictions get blurry when liana abundance is

considered, (3) that variations in TLS and HPs parameters can be used to predict the effect of liana abundance on the successional path, (4) that not all the parameters could address the effect of the presence or impact of lianas along a successional gradient, and (5) we suggest that the impact of lianas on successional stages changes the deterministic nature of forest structure, by randomizing the 3D space where they grow at given plot; the higher the abundance of lianas the higher the randomization.

Our study provides important insights on the contributions of lianas to the successional process, and highlights the potential that TLS has in monitoring liana presence in tropical dry forests environments. Lianas are increasing in density and biomass in tropical forests, but it is unknown whether this pattern is also found in secondary forests, which are suitable for liana proliferation. TLS systems are capable of providing unbiased estimations for the vertical structure of a given site, and thus constitute a powerful tool to monitor the increases in liana density and biomass. Although, our study is limited to one single site in Costa Rica, this is a first step on the development of more comprehensive approaches, which take advantage of advanced technology to understand the effects of liana abundance on tropical dry forest structure. The approach presented in this paper, presents important contributions to efforts directed to estimate the potential effects of lianas on forest carbon in secondary forests (*Durán and Sanchez-Azofeifa, 2015*), elements that seems not fully considered yet in the tropical literature.

Acknowledgements

This work was carried out with the aid of a grant from the Inter-American Institute for Global Change Research (IAI) CRN3 025 which is supported by the US National Science

563 Foundation [Grant GEO-1128040], and the Discovery Grant Program of the National
564 Science and Engineering Research Council of Canada. We thank Ericka James her help
565 during the process of data analysis. We thank also Dr. Stefan Schnitzer for comments on
566 earlier versions of the manuscript and the constructive comments from three anonymous
567 reviewers.
568

569 **References**

570 Arroyo-Mora, J.P., Sánchez-Azofeifa, G.A, Kalacska, M., Rivard, B., Calvo-Alvarado, J.,
571 and Janzen, D.: Secondary forest detection in a Neotropical dry forest landscape
572 using Landsat 7 ETM+ and IKONOS Imagery. Biotropica, 37(4), 497-507, 2005a.
573 Arroyo-Mora, J. P., Sanchez-Asofeifa, G.A, Rivard, B., Calvo-Alvarado, J. C. and Janzen,
574 D. H.: Dynamics in landscape structure and composition for the Chorotega region,
575 Costa Rica from 1960 to 2000, Agriculture, Ecosystems & Environment, 106(1), 27–
576 39, 2005b.
577 Beland, M., Baldocchi, D. D., Widlowski, J.-L., Fournier, R. A. and Verstraete, M. M.: On
578 seeing the wood from the leaves and the role of voxel size in determining leaf area
579 distribution of forests with terrestrial LiDAR, Agriculture and Forest Meteorology
580 184, 82–97, 2014.
581 Calvo-Alvarado, J., B McLennan, GA Sánchez-Azofeifa, and T Garvin.: Deforestation and
582 forest restoration in Guanacaste, Costa Rica: Putting conservation policies in context.
583 For. Ecol. Manage, 258(6), 931-940, 2009.
584 Canty, A. and Ripley B.: boot: bootstrap functions, available at: https://cran.r-
585 project.org/web/packages/boot/ (last access: September 30, 2016), 2016.

586 Cao, S., Yu, Q., Sanchez-Azofeifa, A., Feng, J., Rivard, B., & Gu, Z.: Mapping tropical dry
587 forest succession using multiple criteria spectral mixture analysis. ISPRS Journal of
588 Photogrammetry and Remote Sensing, 109, 17-29, 2015.
589 Castillo, M., Rivard, B., Sánchez-Azofeifa, A., Calvo-Alvarado, J. and Dubayah, R.: LIDAR
590 remote sensing for secondary Tropical Dry Forest identification, Remote Sens.
591 Environ., 121, 132–143, 2012.
592 Castro-Esau, K., Sánchez-Azofeifa, G.A. and Caelli, T.: Discrimination of lianas and trees
593 with leaf-level hyperspectral data, Remote Sens. Environ., 90 (3), 353–372, 2004.
594 Chen, Y.-J., Bongers, F., Cao, K.-F. and Cai, Z.-Q.: Above- and below-ground competition
595 in high and low irradiance: tree seedling responses to a competing liana *Byttneria*
596 *grandifolia*. J. Trop. Ecol., 24, 517–524, 2008.
597 Clawges, R., Vierling, L., Calhoon, M. and Toomey, M.: Use of a ground-based scanning
598 lidar for estimation of biophysical properties of western larch (*Larix occidentalis*),
599 Int. J. Remote Sens. 28 (19), 4331–4344, 2007.
600 Culvenor, D., Newnham, G., Mellor, A., Sims, N. and Haywood, A.: Automated In-Situ
601 Laser Scanner for Monitoring Forest Leaf Area Index, Sensors, 14(8), 14994–15008,
602 2014.
603 Dassot, M., Constant, T. and Fournier, M.: The use of terrestrial LiDAR technology in forest
604 science.: Application fields, benefits and challenges, Ann. For. Sci., 68(5), 959–974,
605 2011.
606 Dewalt, S. J., Schnitzer, S. A. and Denslow, J. S.: Density and diversity of lianas along a
607 chronosequence in a central Panamanian lowland forest, J. Trop. Ecol., 16(1), 1–19,
608 2000.

609 Durán, S.M. and Gianoli, E.: Carbon stocks in tropical forests decrease with liana density,
610 Biol. Lett., 3–6, 2013.
611 Durán, S. M. and Sánchez-Azofeifa.: Liana effects on carbon storage and uptake in mature
612 and secondary tropical forests, in: Biodiversity of lianas, edited by: Parthasarathy, N.,
613 pp. 43–55. Springer-Verlag, 2015.
614 Frazer, G.W., Canham, C.D., and Lertzman, K.P.: Gap light analyzer (GLA), Version 2.0:
615 Imaging software to extract canopy structure and gap light transmission indices from
616 true-colour fisheye photographs, users manual and program documentation. Simon
617 Fraser University, BC and the Institute of Ecosystem Studies, NY, 1999.
618 Foster, J. R., Townsend, P. A. and Zganjar, C. E.: Spatial and temporal patterns of gap
619 dominance by low-canopy lianas detected using EO-1 Hyperion and Landsat
620 Thematic Mapper, Remote Sens. Environ., 112 (5), 2104–2117, 2008.
621 González, I. and Déjean S.: CCA: canonical correlation analysis, available at: https://cran.r-
622 project.org/web/packages/CCA/ (last access: September 30, 2016), 2015.
623 Graham, E. A., Mulkey, S. S., Kitajima, K., Phillips, N. G. and Wright, S. J.: Cloud cover
624 limits net CO2 uptake and growth of a rainforest tree during tropical rainy seasons.,
625 Proc. Natl. Acad. Sci. U. S. A., 100(2), 572–576, 2003.
626 van der Heijden, G.M.F, Schnitzer, S.A., Powers, J.S. and Phillips, O.L.: Liana Impacts on
627 Carbon Cycling, Storage and Sequestration in Tropical Forests. Biotropica 45, 682–
628 692, 2013.
629 van der Heijden, Powers, J.S., and Schnitzer, S.A.: Lianas reduce carbon accumulation and
630 storage in tropical forests. PNAS 112, 13267-13271, 2015.

631 Hilje, B., Calvo-alvarado, J., Jiménez-rodríguez, C., Sánchez-azofeifa, A., José, S., Rica, C.,
632 Forestal, E. D. I., Rica, T. D. C. and Rica, C.: Tree species composition, breeding
633 systems, and pollination and dispersal syndromes in three forest successional stages
634 in a tropical dry forest in Mesoamerica, Trop. Conserv. Sci., 8(1), 76–94, 2015.
635 Jupp, D. L. B., Culvenor, D. S., Lovell, J. L., Newnham, G. J., Strahler, A. H. and
636 Woodcock, C. E.: Estimating forest LAI profiles and structural parameters using a
637 ground-based laser called "Echidna"., Tree Physiol., 29(2), 171–81, 2009.
638 Kalacska, M.: Leaf area index measurements in a tropical moist forest: A case study from
639 Costa Rica, Remote Sens. Environ., 91(2), 134–152, 2004.

640 Kalascka, M., J Calvo, and GA Sánchez-Azofeifa: Assessment of seasonal changes in
641 species' leaf area in a tropical dry forest in different states of succession. Tree
642 Physiology. 25: 733-744. 2005a.

643 Kalacska, M., Sánchez-Azofeifa, G. A., Calvo-Alvarado, J. C., Rivard, B. and Quesada, M.:
644 Effects of season and successional stage on leaf area index and spectral vegetation
645 indices in three mesoamerican tropical dry forests, Biotropica, 37(4), 486–496,
646 2005b.
647 Kalacska, M., Sanchez-Azofeifa, G. A., Rivard, B., Caelli, T., White, H. P. and Calvo-
648 Alvarado, J. C.: Ecological fingerprinting of ecosystem succession: Estimating
649 secondary tropical dry forest structure and diversity using imaging spectroscopy,
650 Remote Sens. Environ., 108, 82–96, 2007a.
651 Kalacska, M., Bohlman, S., Sanchez-Azofeifa, G. A., Castro-Esau, K. and Caelli, T.:
652 Hyperspectral discrimination of tropical dry forest lianas and trees: Comparative data

reduction approaches at the leaf and canopy levels, Remote Sens. Environ., 109, 406–415, 2007b.

Ledo, A., Illian, J. B., Schnitzer, S. A., Wright, S. J., Dalling, J. W. and Burslem, D. F. R. P.: Lianas and soil nutrients predict fine-scale distribution of above-ground biomass in a tropical moist forest, J. Ecol., 104, 1819–1828, 2016.

Lefsky M., and McHale M..: Volumes estimates of trees with complex architecture from terrestrial laser scanning. J Appl Remote Sens., 2, 023521, 2008.

Letcher, S. G. and Chazdon, R. L.: Lianas and self-supporting plants during tropical forest succession, For. Ecol. Manage., 257 (10), 2150–2156, 2009.

Lovell, J. L., Jupp, D. L. B., Culvenor, D. S. and Coops, N. C.: Using airborne and ground-based ranging lidar to measure canopy structure in Australian forests, Can. J. Remote Sens., 29 (5), 607–622, 2014.

Menzel, U.: CCP: Significance tests for canonical correlation analysis (CCA), available at: https://cran.r-project.org/web/packages/CCP/ (last access: September 30, 2016), 2012.

Muss, J. D., Aguilar-Amuchastegui, N., Mladenoff, D. J. and Henebry, G. M.: Analysis of Waveform Lidar Data Using Shape-Based Metrics, IEEE Geosci. Remote Sens. Lett., 10 (1), 106–110, 2013.

Paul, G. S. and Yavitt, J. B.: Tropical Vine Growth and the Effects on Forest Succession: A Review of the Ecology and Management of Tropical Climbing Plants, Bot. Rev., 77 (1), 11–30, 2010.

Phillips, O., Martínez, R., Arroyo, L. and Baker, T.: Increasing dominance of large lianas in Amazonian forests, Nature, 418, 770–774, 2002.

676 Phillips, O. L. and Lewis, S. L.: Recent changes in tropical forest biomass and dynamics,
677 For. Glob. Chang., 4, 77–108, 2014.
678 Phillips, O. L., Vásquez Martínez, R., Monteagudo Mendoza, A., Baker, T. R. and Núñez
679 Vargas, P.: Large lianas are hyperdynamic elements of the tropical forest canopy,
680 Ecology, 86, 1250–1258, 2005.
681 Portillo-Quintero, C., Sanchez-Azofeifa, A. and Culvenor, D.: Using VEGNET In-Situ
682 monitoring LiDAR (IML) to capture dynamics of plant area index, structure and
683 phenology in Aspen Parkland Forests in Alberta, Canada, Forests, 5 (5), 1053–1068,
684 2014.
685 Poulsen, J. R., Koerner, S. E., Miao, Z., Medjibe, V. P., Banak, L. N. and White, L. J. T.:
686 Forest structure determines the abundance and distribution of large lianas in Gabon,
687 Glob. Ecol. Biogeogr., doi:10.1111/geb.12554, 2016.
688 Quesada, M., Sanchez-Azofeifa, G. A., Alvarez-Añorve, M., Stoner, K. E., Avila-Cabadilla,
689 L., Calvo-Alvarado, J., Castillo, A., Espírito-Santo, M. M., Fagundes, M., Fernandes,
690 G. W., Gamon, J., Lopezaraiza-Mikel, M., Lawrence, D., Morellato, L. P. C., Powers,
691 J. S., Neves, F. D. S., Rosas-Guerrero, V., Sayago, R. and Sanchez-Montoya, G.:
692 Succession and management of tropical dry forests in the Americas: Review and new
693 perspectives, For. Ecol. Manage., 258 (6), 2009.
694 Quinn, G. P. and Keough M. J.: Experimental design and data analysis for biologists.
695 Cambridge University Press, New York, 443-472, 2002.
696 R Development Core Team: R: a language and environment for statistical computing,
697 available at: http://www.r-project.org (last access: September 30, 2016), 2016.

698 Ramírez, F. A., Armitage, R. P. and Danson, F. M.: Testing the application of terrestrial
699 laser scanning to measure forest canopy gap fraction, Remote Sens., 5 (6), 3037–
700 3056, 2013.
701 Richardson, J., Moskal, L. and Bakker, J.: Terrestrial Laser Scanning for Vegetation
702 Sampling, Sensors, 14 (11), 20304–20319, 2014.
703 Sánchez-Azofeifa, RC Harris, and DL Skole. Deforestation in Costa Rica: A quantitative
704 analysis using remote sensing imagery. Biotropica. 33(3), 378-384, 2001.
705 Sánchez-Azofeifa, G. A. and Castro-Esau, K.: Canopy observations on the hyperspectral
706 properties of a community of tropical dry forest lianas and their host trees, Int. J.
707 Remote Sens., 27 (10), 2101–2109, 2006.
708 Sánchez-Azofeifa, G. A., Kalácska, M., Espírito-Santo, M. M. Do, Fernandes, G. W. and
709 Schnitzer, S.: Tropical dry forest succession and the contribution of lianas to wood
710 area index (WAI), For. Ecol. Manage., 258 (6), 941–948, 2009.
711 Schnitzer, S. A and Bongers, F.: Increasing liana abundance and biomass in tropical forests:
712 emerging patterns and putative mechanisms., Ecol. Lett., 14 (4), 2011.
713 Schnitzer, S. A and Carson, W. P.: Lianas suppress tree regeneration and diversity in treefall
714 gaps., Ecol. Lett., 13 (7), 849–57, 2010.
715 Schnitzer, S. A., Dalling, J. W. and Carson, W. P.: The impact of lianas on tree regeneration
716 in tropical forest canopy gaps: evidence for an alternative pathway of gap-phase
717 regeneration, J. Ecol., 88 (4), 655–666, 2000.
718 Schnitzer, S., van der Heijden, G.M.F., and Powers, J.: Addressing the challenges of
719 including lianas in global vegetation models. PNAS, 113 (1), E6, 2016.

720 Schnitzer, S. A., van der Heijden, G., Mascaro, J. and Carson, W. P.: Lianas in gaps reduce
721 carbon accumulation in a tropical forest, Ecology, 95, 3008–3017, 2014.
722 Strahler, A. H., Jupp, D. L. ., Woodcock, C. E., Schaaf, C. B., Yao, T., Zhao, F., Yang, X.,
723 Lovell, J., Culvenor, D., Newnham, G., Ni-Miester, W. and Boykin-Morris, W.:
724 Retrieval of forest structural parameters using a ground-based lidar instrument
725 (Echidna ®), Can. J. Remote Sens., 34 (sup2), S426–S440, 2014.
726 Tymen, B., Réjou-Méchain, M., Dalling, J. W., Fauset, S., Feldpausch, T. R., Norden, N.,
727 Phillips, O. L., Turner, B. L., Viers, J. and Chave, J. Evidence for arrested succession
728 in a liana-infested Amazonian forest. J. Ecol. 104 (1), 149-159. 2016.
729 Verbeek, H., Kearsley, E.: The importance of including lianas in global vegetation models,
730 PNAS, 113 (1), E4, 2016.
731 Wright, S. J.: Tropical forests in a changing environment, Trends Ecol. Evol., 20(10), 553–
732 560, 2005.
733 Zhang, J., Rivard, B., Sánchez-Azofeifa, A. and Castro-Esau, K.: Intra- and inter-class
734 spectral variability of tropical tree species at La Selva, Costa Rica: Implications for
735 species identification using HYDICE imagery, Remote Sens. Environ., 105, 129–141,
736 2006.
737

738 Table 1. Mean (± SD) of parameters of forest structure extracted from plots with
739 different successional stages and different relative abundance of lianas in the dry forest
740 at Santa Rosa National Park, Costa Rica. Significant differences (*F-values* and their *p-*
741 *values*) according to the successional stages, relative abundance of lianas and their
742 interaction are represented by a posteriori ANOVA text extracted from MANOVA. Stem
743 density (stems/ha); DBH_{mean}, mean stem diameter at breast height (cm); TBA, total basal
744 area (m^2); L/TBA, ratio of liana basal area to TBA.

Parameters	Early		Intermediate		ANOVA		
	LL	HL	LL	HL	Stage	Condition	Interaction
Stem density	1054 ± 370.72	1218.33 ± 603.24	1027.14 ± 379.02	1021 ± 331.54	0.55	0.15	0.27
DBH_{mean}	10.91 ± 2.36	11.83 ± 1.57	14.17 ± 1.85	11.56 ± 1.89	2.72	2.73	5.65*
TBA	1.44 ± 0.90	2.08 ± 1.01	2.61 ± 0.80	1.84 ± 0.61	1.39	0.48	5.15*
L/TBA (10^{-2})	0.38 ± 0.35	1.48 ± 0.84	0.35 ± 0.32	2.93 ± 2.14	2.76	14.11***	1.86

745 *, $p < 0.05$; ***, $p < 0.01$

746

747 Table 2. Mean (± SD) of parameters calculated by VEGNET system and HPs in plots
748 with different successional stages and different relative abundance of lianas in the dry
749 forest at Santa Rosa National Park, Costa Rica. Significant differences (*F-values* and
750 their *p-values*) according to the successional stages, relative abundance of lianas and
751 their interaction are represented by a posteriori ANOVA text extracted from MANOVA.
752 RG, radius of gyration; PAI, plant area index; $PAVD_{mean}$, plant area volume density;
753 H_{max}, maximum tree height (m); LAI, leaf area index.

Parameters	Early		Intermediate		ANOVA		
	LL	HL	LL	HL	Stage	Condition	Interaction
RG	4.21 ± 1.42	4.85 ± 0.92	4.69 ± 1.11	4.34 ± 0.91	0.03	0.01	1.41
C_x	0.19 ± 0.06	0.13 ± 0.04	0.14 ± 0.03	0.16 ± 0.04	0.12	0.14	5.95*
C_y	7.56 ± 2.96	8.43 ± 1.63	8.22 ± 2.07	7.56 ± 1.59	0.07	0.01	0.96
PAI	2.45 ± 0.28	2.10 ± 0.28	2.13 ± 0.34	2.31 ± 0.33	0.06	0.05	4.75*
$PAVD_{mean}$	0.19 ± 0.05	0.13 ± 0.04	0.14 ± 0.03	0.16 ± 0.04	0.14	0.22	7.26*
H_{max}	17.42 ± 5.51	18.17 ± 3.90	23.26 ± 7.73	18.01 ± 6.00	0.99	1.53	1.61
LAI	2.30 ± 0.32	2.46 ± 0.64	2.34 ± 0.46	2.92 ± 0.39	2.97	6.91*	1.32
Canopy openness	13.90 ± 3.94	12.59 ± 5.89	12.74 ± 5.27	8.67 ± 1.47	5.77*	6.78*	0.79

754 *, $p < 0.05$

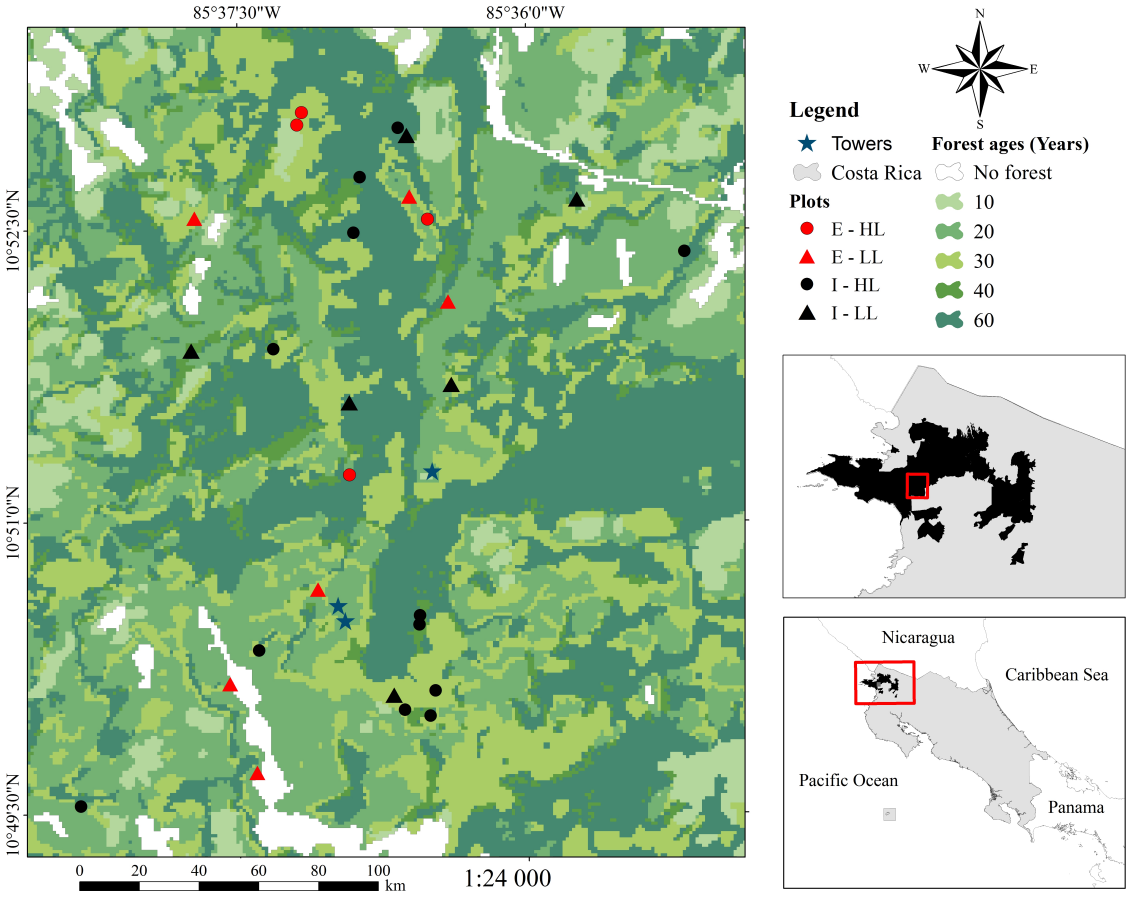

Figure 1. Localization of the sampled forest stands in Santa Rosa National Park Environmental Monitoring Super Site, Guanacaste, Costa Rica. Where E-HL indicate Early successional stage with a high relative abundance of lianas; E-LL Early successional stage with a low relative abundance of lianas; I-HL, Intermediate successional stage with a high relative abundance of lianas; I-LL, Intermediate successional stage with a low relative abundance of lianas. In addition, forests ages refer to: 60, forests detected since 1956; 40, forests detected since 1979; 30, forests detected since 1986; 20, forests detected since 1997; 10 forests detected since 2005, and no forest correspond to non-related to woodlands.

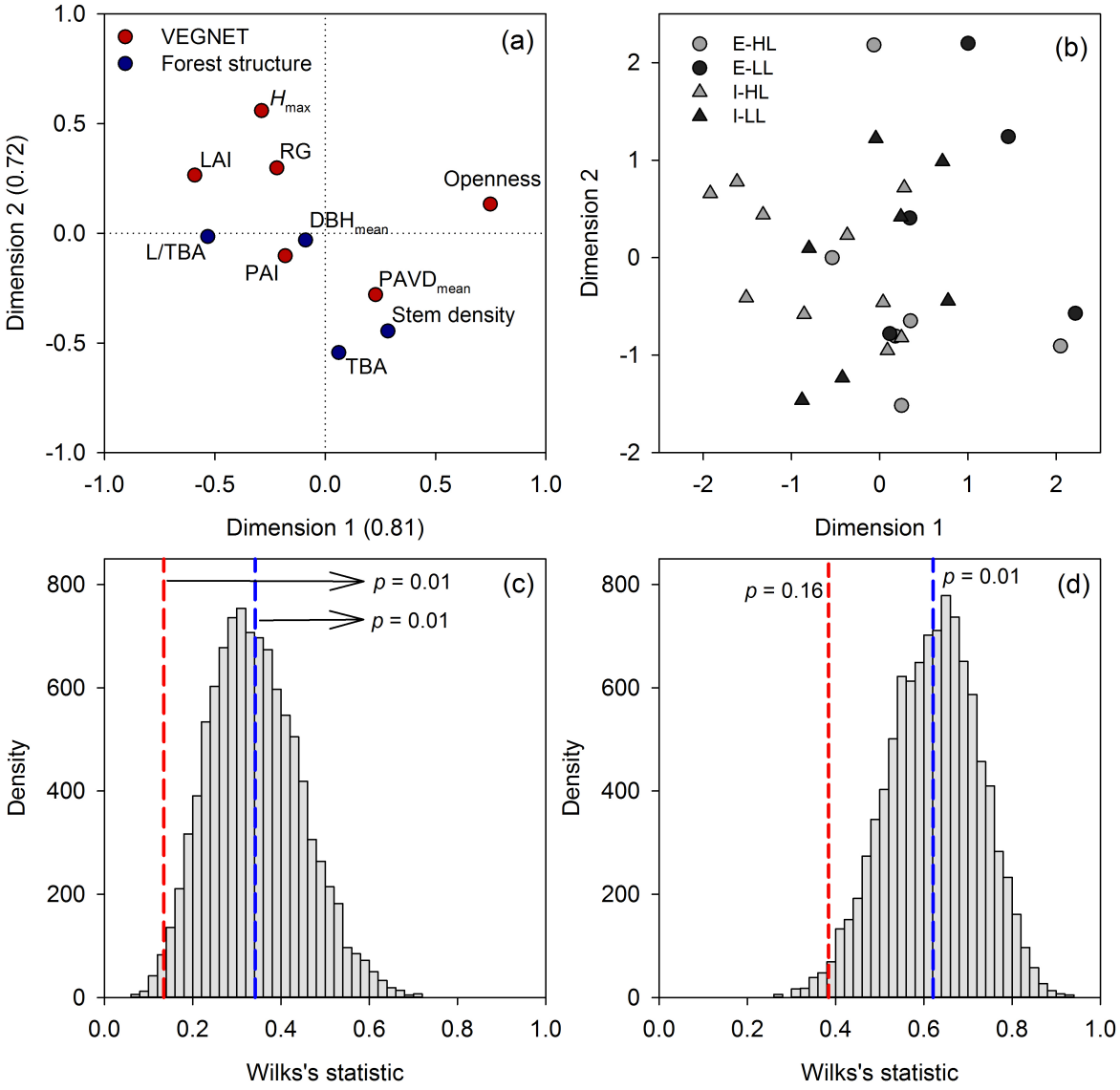

767

768 Figure 2. Canonical correspondence analysis to describe the association between the
769 parameters estimated by VEGNET system-hemispherical photographs (HPs) and the
770 forest structure. a) VEGNET-HPs coefficients are represented by red points, while forest
771 structure coefficients are represented by blue points. b) Individual scores of each plot of
772 the canonical variates are represented according to successional stages (E, early; I,
773 intermediate) and relative liana abundance (LL, low liana abundance; HL, high liana
774 abundance). C and d represent the permutation distribution of the Wilks' Lambda test to

775 assign the statistical significance of canonical correlation coefficients considering 4 and
776 3 canonical correlations, respectively; the red line represent the original value Wilks'
777 Lambda, while the blue line represent the mean value permutated.
778

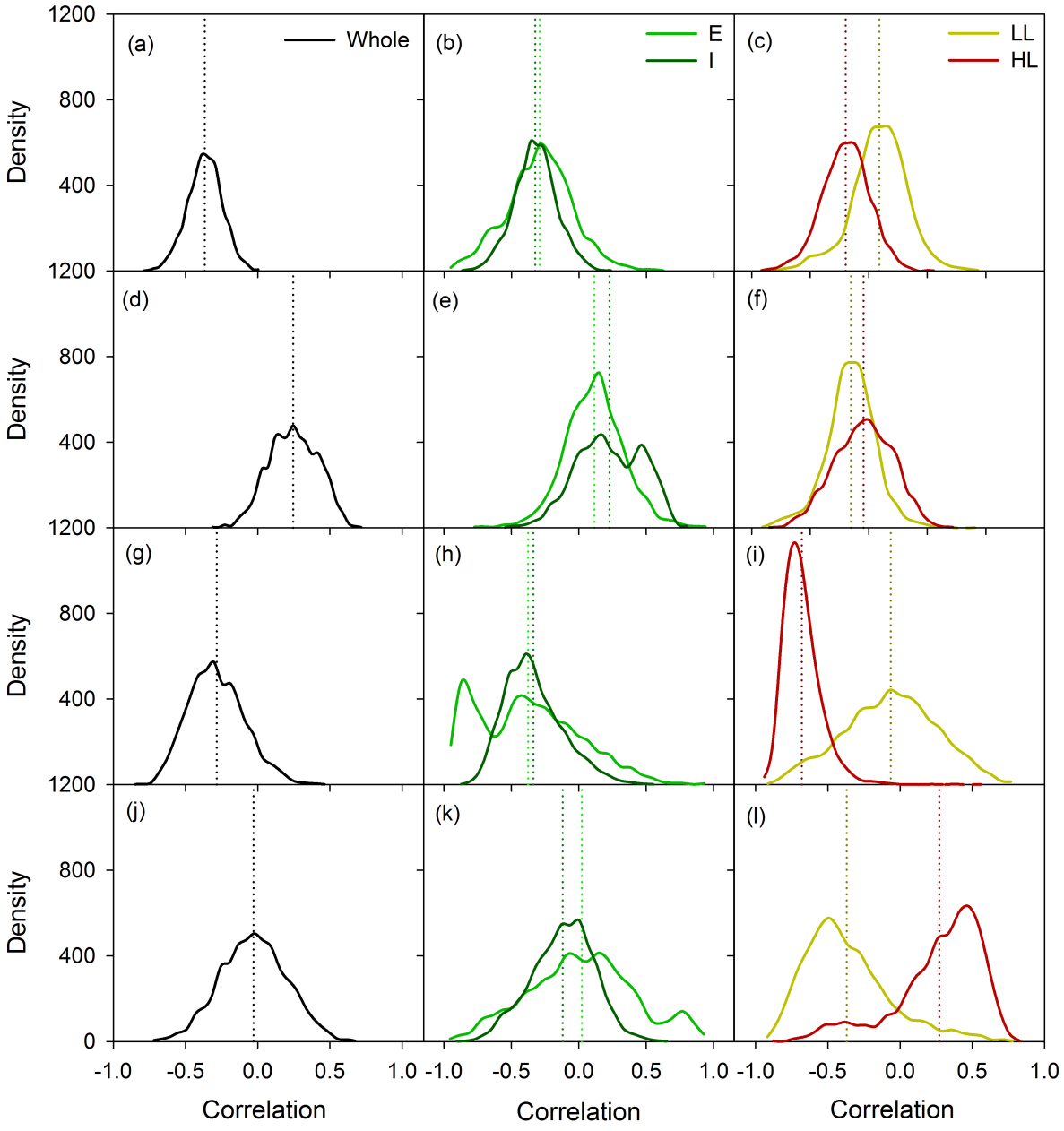

779

780 Figure 3. Density distribution of the bootstrapped correlation coefficients without and
781 with distinction between successional stages (E, early; I, intermediate) and relative liana
782 abundance (LL, low liana abundance; HL, high liana abundance). a, b, and c correspond
783 to the correlation of canopy openness and the ratio of liana basal area (L) to total basal
784 area (TBA); d, e, f correspond to leaf area index-L/TBA correlation; g, h, and i

785 correspond to the maximum tree height-TBA correlation; j, k, and l correspond to plant
786 area volume density-TBA correlation.